

<https://helda.helsinki.fi>

Wind and gravity in shaping Picea trunks

Larjavaara, Markku

2021-10

Larjavaara , M , Auvinen , M , Kantola , A & Makela , A 2021 , ' Wind and gravity in shaping Picea trunks ' , Trees : Structure and Function , vol. 35 , pp. 1587-1599 . <https://doi.org/10.1007/s00468-021-02138-3>

<http://hdl.handle.net/10138/343395>

<https://doi.org/10.1007/s00468-021-02138-3>

other

acceptedVersion

Downloaded from Helda, University of Helsinki institutional repository.

This is an electronic reprint of the original article.

This reprint may differ from the original in pagination and typographic detail.

Please cite the original version.

1 Original Article

2

3 **Wind and gravity in shaping *Picea* trunks**

4

5 Markku Larjavaara^{1*}, Mikko Auvinen², Anu Kantola³, Annikki Mäkelä⁴

6

7 ¹ Institute of Ecology and Key Laboratory for Earth Surface Processes of the Ministry of
8 Education, College of Urban and Environmental Sciences, Peking University, Beijing
9 100871, China

10 ² Atmospheric Dispersion Modelling, Atmospheric Composition Research, Finnish
11 Meteorological Institute, Finland

12 ³ Natural Resources Institute Finland (Luke), P.O.Box 2 (Latokartanonkaari 9), FI-00791
13 Helsinki, Finland

14 ⁴ Department of Forest Sciences, P.O.Box 27 (Latokartanonkaari 7), 00014 University of
15 Helsinki, Finland

16

17 * Corresponding author (markku@pku.edu.cn)

18 **Abstract**

19 Understanding why trunks (tree stems) are the size that they are is important. However, this
20 understanding is fragmented into isolated schools of thought and has been far from complete.
21 Realistic calculations on minimum trunk diameters needed to resist bending moments caused
22 by wind and gravity would be a significant step forward. However, advancements using this
23 biomechanical approach have been delayed by difficulties in modelling bending of trunks and
24 wind gusts. We felled and measured five Norway spruces (*Picea abies*) in an unthinned
25 monoculture in southeastern Finland planted 67 years earlier. We then focused on forces
26 working on storm-bent (maximally bent) trees caused by gravity and the strongest gust in a
27 one-hour simulation with a large-eddy simulation model. The weakest points along the trunks
28 of the three largest trees resisted mean above-canopy wind speeds ranging from 10.2 m s⁻¹ to
29 12.7 m s⁻¹ (3.3-fold in the strongest gust), but the two smallest were well protected by a dense
30 layer of leaves from the bending tops of larger trees, and could have resisted stronger winds.
31 Gravity caused approximately one quarter of the critical bending moments. The wind that
32 breaks the trunks in their weakest points is close to breaking them in other points, supporting
33 importance of bending moments caused by wind and gravity in evolution of trunk taper.

34

35 **Keywords**

36 Gravity, Norway spruce (*Picea abies* [L.] Karst.), Sail area, Stem, Thigmomorphogenesis,
37 Trunk taper, Wind drag, Wood

38

39 **Key Message**

40 Spruce trunk tapering corresponds closely to tapering required to resist bending forces caused
41 by wind and gravity.

42 **Introduction**

43

44 Understanding why trees and their trunks (stems) are the size that they are is important for
45 evaluating the potential of forests to mitigate climate change and produce timber. Therefore it
46 is surprising that that the scientific understanding of tree height and diameters along the trunk
47 is fragmented. For example, a question concerning the dimensional determinants of a
48 particular tree trunk may cause surprise and be considered too general by experts in narrow
49 fields, even though understanding trunk dimensions should be considered one of the largest
50 questions in applied ecology.

51

52 Research on trunk dimensions can be classified in two ways. Firstly, the classification can be
53 based on the object of the study, i.e. the state of the forest. Some studies focus on those
54 experiencing natural successions (Anderson-Teixeira et al., 2013), others on tallest trees in
55 old-growth forests (Van Pelt et al., 2016), on plantations subject to self-thinning (Yoda et al.,
56 1963) or impacts of silvicultural treatments (Bianchi et al., 2020). Secondly, the classification
57 can be based on whether the approach is descriptive or theoretical. The majority of research
58 on trunk dimensions in forest sciences and research related to forests' role in climate change
59 mitigation is mainly descriptive (e.g. Chave et al., 2014), while much of the physiological
60 and ecological research attempts to explain the causes of the described patterns based on
61 theories. These theories may be grouped based on the function on which the focus is:
62 transport, storage or biomechanical support as explained in the following paragraphs.

63

64 Trees passively transport sap (water) up in the sapwood, and the resistance caused by length
65 of the path or need to lift sap against gravity has been used as the basis for modelling
66 maximum tree height (Koch et al., 2004) and growth deceleration in plantations (Ryan and

67 Yoder, 1997). However, as the heartwood is not contributing to sap transport, diameters
68 along the trunk cannot be understood based on sap transport only, unless heartwood is
69 considered a waste produced e.g. due to ageing (Collalti et al., 2019) or difficulties in using
70 the same sapwood when branches die and grow (Chiba et al., 1988). Phloem transport down
71 the trunk may be similarly limiting tree height due to path length (Woodruff, 2013), but
72 again, does not explain diameters, unless trunk circumference needs to be increased to
73 increase transport capacity.

74

75 Trees store water (Scholz et al., 2011) and energy (Schiestl-Aalto et al., 2015) in their woody
76 tissues and this is likely to influence trunk dimensions in certain conditions. For example,
77 baobab (*Adansonia digitata*) trees probably have unusually fat trunks to store water needed to
78 level out seasonal variation in water availability (Chapotin et al., 2006), and lignotubers
79 located at the trunk base can store energy and nutrients enabling rapid sprouting (Canadell
80 and López-Soria, 1998). Trunk dimensions are therefore potentially influenced by storage
81 needs, but this is unlikely to be common and may be restricted to the rare trees that do not
82 form metabolically dead heartwood and therefore cannot increase sapwood volume by
83 adjusting the sapwood-to-heartwood-ratio such as the above-mentioned baobabs (Patrut et al.,
84 2010).

85

86 The third general function of trunks in addition to transport and storage, and the only for
87 which heartwood is useful, is to biomechanically support the leaves, branches and trunk
88 sections above the height at which the focus is. Common sense tells that trees exposed to
89 wind or heavy loads need to have thicker trunks for a given height and crown size. These
90 mechanism have been studied experimentally for over two centuries (Telewski, 2016), and
91 the term “thigmomorphogenesis” has become established in the recent decades to describe

92 the responses of plants to mechanical stimuli (Pruyn et al., 2000). Two very different
93 mechanisms may serve as a basis for modelling trunk dimensions biomechanically. Elastic
94 buckling (Euler buckling) can permanently bend trunks if the tree fresh mass and permanent
95 loads, such as epiphytes and lianas, exceed the limit that the trunk can support. Modelling can
96 be performed easily (McMahon, 1973), and normally a “safety factor” is computed
97 describing how far the height of the tree is from a height that leads to buckling. This approach
98 has been used in well-known modelling approaches (e.g. West et al., 1999). However, most
99 trees, with the exception of certain rainforest understorey trees, are far from elastic buckling.
100 For example, Niklas (1994) reported an average safety factor of four. Because of non-
101 linearities, a safety factor of four implies that plants weight is only 1.6% of the weight that
102 would lead to elastic buckling. Furthermore, the safety factor is a misleading concept and
103 should not be interpreted as an indication of biomechanical safety. A safety margin is needed
104 for engineer-designed structures, as they are built and then need to resist variable forces
105 without subsequent adjustments to the structure. However, thanks to thigmomorphogenesis,
106 trees can tune their structure (Bonnesoeur et al., 2016) and a small safety factor is therefore
107 not dangerous, as supporting tissue can be increased according to demand from the increasing
108 height or weight. The wide usage of the theory on elastic buckling shocked Mattheck (2012)
109 and he wrote: “Much to the surprise of the author, failure by buckling has nevertheless been
110 discussed by McMahon (1973), and comparisons have been made between measured height-
111 diameter relations and relations calculated from Euler's buckling theory." The other, more
112 useful, biomechanical approach is based on trunks breaking. Brief buckling e.g. due to a
113 temporary load of snow may not be a problem for the tree if it recovers and is erect most of
114 the time. However, when modelling trunk breakage, even a short period to which the tree has
115 not been able to acclimatize may be fatal. This modelling approach is challenging to follow,
116 as wind speeds are variable in space and time, and trunks, branches and leaves streamline in

117 wind. In both buckling and breaking approaches, diameters needed along the trunk for a
118 given height and other characteristics can be computed based on biomechanics. However,
119 these approaches do not limit height if the diameters are not limited.

120

121 All trees need trunks to transport, to provide biomechanical support and probably also to
122 store, and theories and modelling to understand trunk dimensions should ideally incorporate
123 all of these with appropriate weights. However, in practice realistic modelling of even one of
124 these aspects at a time is challenging. Therefore, it is useful to consider their relative
125 importance. One challenge is that scientists are typically experts on only one of these three
126 functions and may therefore overestimate its importance, even though some reviews on all
127 them are available (Badel et al., 2015). Secondly, if building or maintaining a trunk that is
128 superior in any of the three functions causes an energetic cost, all functions would evolve
129 close to the needed level even if the cost improving it relative to the others would be
130 minuscule. An example with an engineer-designed product demonstrates this issue well. An
131 expert focusing on tires claims that the speed rating of tires determines the maximum speed
132 of the car, while an engine expert argues that engine power is pivotal. Both would be
133 technically correct, but to understand the main reason why markets set the top speed at its
134 level, the challenges in designing, manufacturing, maintaining and operating engines and tires
135 that allow faster speeds must be considered. This reveals that, as increasing the speed rating
136 of tires is very easy relative to increasing the engine power, and it makes normally more
137 sense to say that the car does not go faster because the engine is not more powerful and not
138 because of its tires. Similarly, demonstrating that e.g. transporting sap higher than the current
139 height of the tallest trees (Koch et al., 2004) does not necessarily mean that sap transport is
140 the main factor determining maximum heights. Instead, in evolutionary time scales for

141 example sap transport capacity could improve to a height determined mainly by the
142 biomechanics and energetics of maintaining the living biomass.

143

144 We did not properly assess the relative importance of how the functions of trunks influence
145 their dimensions, as that would need to be done by incorporating them into one model. In this
146 paragraph, we just note a few pieces of evidence that indicated to us the direction to take.

147 One approach is to consider the marginal construction and maintenance costs of increasing
148 capacity. Tissue suitable for storage or sap transport may be increased by increasing sapwood
149 to heartwood ratio. Furthermore, sap transport efficiency may be boosted without
150 compromising transport safety by increasing the density of conduits in angiosperm wood,
151 probably with little or no additional construction costs (Larjavaara, 2021) . However,
152 significant strengthening of the trunk is not possible without substantial additional
153 construction costs, either by increasing diameters or wood density (Larjavaara and Muller-
154 Landau, 2012).

155

156 Another approach to know about the relative importance of factors influencing trunk
157 dimensions is to compare them in variable environmental conditions that demand for variable
158 transport, storage and biomechanical support needs. This approach underlines the importance
159 of sap transport if height and diameters along the trunk vary according to water availability.

160 The very tallest trees would then be expected to be found in climates and soils with most
161 abundant water, which is not the case, even though the driest climates have a low canopy
162 height (Klein et al., 2015). If storage function was critical in determining trunk dimensions,
163 then seasonality should increase trunk volumes relative to leaf area, which may be the case
164 (Chapotin et al., 2006) but probably only in the case of exceptional species. Finally, with
165 biomechanical support being the most significant, tree heights and forest biomasses should

166 vary depending on winds. This is the case for example with variable distances from the edge
167 and therefore variable wind regimes (Brüchert and Gardiner, 2006). Another perspective on
168 the importance of biomechanics is provided by comparing trees to lianas, which do not have
169 the same biomechanical support needs. Lianas have similar transport and storage needs as
170 trees, and much higher leaf area for a given stem basal area (Ichihashi and Tateno, 2015),
171 which is very likely due to differing biomechanical needs, highlighting their importance to
172 trunk diameters. These considerations led us to explore the role of wind forces and gravity as
173 key determinants of trunk diameters, which is the focus of this article.

174

175 The importance of wind and gravity as a cause of trunk breakage is perhaps what common
176 sense would suggest to be the main factor explaining trunk dimensions. This approach was
177 pioneered in the 19th century (Metzger, 1893) and regularly discussed from perspectives
178 described with keywords such as “uniform stress model” (Mäkelä, 2002) and
179 thigmomorphogenesis when the focus is on the formation of the tissue leading to this uniform
180 stress (Pruyn et al., 2000). However, we argue that it still remains underrepresented and that
181 this is probably due to methodological challenges from variable winds. In addition, the
182 streamlining mentioned above and the rarity of the strongest storms that are critical for tree
183 survival and therefore probably drive evolution cause extra challenges. Interesting studies are
184 available on small trees secured on the roof of a moving car (Butler et al., 2012) and medium-
185 sized trees during the leafless period (Niklas and Spatz, 2000), but small (Larjavaara, 2015)
186 and leafless (Mattheck, 2000) trees have different biomechanical constraints than large
187 foliated trees. Large foliated trees have also been examined in impressive studies representing
188 simple (Morgan and Cannell, 1994), more realistic (Spatz and Bruechert, 2000) or excellent
189 detail in tree dimensions (Jackson et al., 2019). However, none of these studies focused on
190 maximally bent trees.

191

192 The objective of this study was to increase our comprehension of determinants concerning
193 tree size and trunk taper, as modified by selective pressures caused by exposure to storm-
194 strength winds, and to examine whether trees are adapted and acclimatized via
195 thigmomorphogenesis to those. To this end, we modelled wind in a canopy of a mature
196 storm-bent stand and computed gravity- and wind-caused forces on segments along the trunks
197 based on destructive sampling of *Picea abies* [L.] Karst. trees (Norway spruces). We then
198 focused on the winds that break the trunks at their weakest segment and expected diameters
199 at other segments to be only slightly larger than what was needed to resist the bending
200 moments caused by this wind and gravity.

201

202

203 **Methods**

204

205 *Picea abies* is a common tree species in its natural range of Northern Europe and Central
206 European mountains and is also planted widely in Central European lowlands and North
207 America (Caudullo et al., 2016). In Finland, *Picea abies* trunk volumes make up 30% of all
208 tree trunk volumes and the volume of harvested trees is 38% of total (Peltola, 2014). It
209 regenerates in intermediate or fertile soils, is the most shade tolerant of the common tree
210 species in Finland and will therefore invade all but the most infertile sandy or peat soils when
211 sufficient time since disturbance has passed (Kuuluvainen and Aakala, 2011). *Picea abies*
212 trees have a straight trunk and long conical crown often reaching the ground. In Finland, the
213 lower branches shed normally only from the lower crown layers in the deep shade of
214 conspecifics. New branches develop annually, forming whorls of branches. Its wood is of low

215 density at 374 kg m^{-3} (Kantola and Makela, 2006) especially when compared to angiosperms
216 (Chave et al., 2009).

217

218 We based our study on data collected in 2001 to investigate crown development in three sites
219 around southern Finland in stands after canopy closure (Kantola and Mäkelä, 2004).

220 However, to reduce the complexity of wind gust-related analysis, only a single plot featuring
221 flat terrain is included in this study. The other plots were excluded because of hilly terrain,
222 which alters low-altitude winds in a complex manner (Gardiner et al., 2016). The included
223 plot, described in more detail by Kantola and Mäkelä (2004), was located in Punkaharju
224 municipality at $61^{\circ}49'N$, $29^{\circ}19'E$, now part of Savonlinna in southeastern Finland. The local
225 climate is conducive to tree growth, as abundant lakes level out temperature fluctuations
226 during the growing season. The soils in the plot are well above average fertility for the
227 region, classified as *Oxalis*-type (Cajander, 1949), leading to a site index, H_{100} of 32 m. The
228 monoculture of *Picea abies* trees was planted 67 years prior to data collection.

229

230 Three stands with varying thinning histories were studied in the plot but two were excluded
231 from our study because of thinnings, as explained below. The included unthinned stand had a
232 basal area of $44 \text{ m}^2 \text{ ha}^{-1}$ and stand density of 805 ha^{-1} . Five sample trees representing various
233 canopy layers were felled, and their trunks, branches and leaves (i.e. needles) were measured
234 and weighed as described in detail by Kantola and Mäkelä (2004). In summary, trunk
235 diameters were measured below each whorl of branches, and all branches were cut and
236 measured and a subset of them taken to a laboratory for more detailed measurements. The
237 heights and diameters of the five trees at a 1.3-m height ($d_{1.3}$) can be seen in Fig. 8 in the
238 Results section. The percentage of the trunk with living branches of the five sample trees
239 differed between 42–63, being greatest for dominant trees and smallest for trees grown in

240 more suppressed positions. And further, the more suppressed trees also had the lightest-
241 weight crowns compared to more dominant ones, which was consistent with the pipe model
242 theory (Kantola and Mäkelä, 2004).

243

244 For this study, we divided the five tree trunks into “segments” and estimated their angle
245 relative to vertical and location relative to the base based on bending and length of all
246 segments below. From the angle relative to vertical we computed their projected area
247 perpendicular to wind direction (i.e. frontal area) and fresh mass based on volumes. We
248 assumed the centre of each segment to be in the whorl of branches and extremes to be located
249 half way between neighbouring whorls. We divided the unmeasured lower branchless trunk
250 into four segments, with the lowest centred at a height of 1.3 m, the remaining three at regular
251 intervals between 1.3 m and the lowest whorl and assumed diameter to simply change
252 linearly, as we anticipated this lowest part of the trunk to contribute only little to the bending
253 moments or to the bending of the trunk.

254

255 The streamlining of trees is complex, and therefore the common approach is to simulate
256 upright trees but with reduced wind drag estimated with a coefficient (Gardiner et al., 2016).
257 We instead focused on the strongest gust and “storm-bent” trees, i.e. trees bent along their
258 trunks as much as they can without breaking (see Fig. 6). This focus was based on the
259 reasoning that even though acclimation is likely to be mainly driven via
260 thigmomorphogenesis by signals from normal wind speeds (Bonnesoeur et al., 2016), trunks
261 are probably tuned to resist the strongest gusts based on normal winds. Maximum strain in
262 both compression and tension may be assumed to equal the ratio of modulus of rupture and
263 modulus of elasticity (but see Niez et al., 2019). In a bending segment or cylinder, the
264 maximum tension occurs in the outermost fibres of the convex side and maximum

265 compression on the opposite side. However, to simplify the calculations, we assumed rigidity
266 of the segments (as can be seen in Fig. 3) and bending was realised by assuming a change (α)
267 in the deviation of the axis of the segment relative to the segment below:

268

$$\alpha = \sin^{-1} \frac{2l\sigma}{dE} \quad (1)$$

269

270 where l is the length of the segment, σ the modulus of rupture obtained from tree-pulling
271 experiment is 36.26 Mpa (Peltola et al., 2000), d the diameter of the segment at its centre and
272 E the modulus of elasticity is 7730 Mpa (Peltola et al., 2000).

273

274 We used the projected area of trunks, branches and leaves (we call their sum “sail area”) first
275 for estimating wind speeds and then to compute wind-caused horizontal forces (Online
276 Resource 1).

277

278 In addition to the five felled trees, we measured the $d_{1.3}$ of all trees less than seven metres
279 away from the felled ones. We estimated their sail area and its vertical storm-bent distribution
280 by fitting two simple linear regressions to the variables. We then first computed the storm-
281 bent height based on the model in Fig. 1 and then its sail area based on the model in Fig. 2, in
282 which a linear relationship was expected based on biomechanics, as the bending moment is
283 expected to scale roughly with the product of the sail area and the length of the lever (tree
284 height) and the strength of the trunk with the cube of its diameter (Ennos, 2012). We plotted
285 these models for all three stands, but observed the fit to be tight in the unthinned plot only.
286 We surmised that as the previous thinning occurred only 14 years prior to the measurement,
287 the trunk dimensions relative to the sail area (Online Resource 1, Fig. S1 and S2) were

288 possibly still unbalanced because of too little time since the thinning. We therefore excluded
289 these stands from the analysis.

290

291 The mean $d_{1,3}$ of the five felled trees was 0.272 m and they ranged from 0.213 m to 0.328 m,
292 while the surrounding trees around these five had a mean of 0.260 m and a range from 0.167
293 m to 0.382 m. Because of the tight fit of models in Fig. 1 and Fig. 2, we do not think that
294 extrapolating to some distance out of the range was likely to cause a significant bias.

295

296 We wanted to focus on strongest wind gusts that the trees can stand and therefore used
297 turbulence resolving large-eddy simulation (LES) model to describe wind behaviour above
298 and within forest canopies. Because of significant horizontal movement of trees in gusts we
299 had to assume that the forest canopy had a horizontally homogenous sail area and therefore
300 sail area per unit volume (i.e. plant area density) for each 1.5-m thick layer. The large-eddy
301 simulation model PALM (Maronga et al., 2015) was employed to obtain a time-accurate and
302 spatially resolved description of fully developed boundary layer turbulence over continuous
303 forest canopy. The PALM model is specifically tailored for atmospheric boundary layer
304 turbulence applications and has been optimized for massively parallel supercomputing
305 environments. The model implements the conservation equations governing atmospheric
306 boundary layer turbulence employing finite-difference discretization on a staggered Cartesian
307 grid. The system of equations is solved using a third-order accurate Runge-Kutta time-
308 stepping scheme and fifth-order accurate upwind biased spatial discretization scheme
309 (Wicker and Skamarock, 2002). The forest canopy is modelled assuming a porous
310 homogenous medium within each 1.5-m layer, whose porosity varies according to the
311 measured vertical sample-averaged plant area density distribution of the trees.

312

313 A vast majority of the drag caused by the forest canopy was assumed to be pressure drag, and
314 therefore the drag force (f) is implemented in PALM as:

315

$$\vec{f} = C_d P |\vec{u}| \vec{u}, \quad (2)$$

316

317 where C_d is the drag coefficient for forest canopy, P is the vertical plant area density profile
318 of the forest, and \vec{u} is the spatially and temporally resolved wind velocity vector whose
319 magnitude is denoted as $|\vec{u}|$. We set C_d at 0.2 as suggested by Katul (1998). The wind
320 simulations were performed on a rectangular domain with L_x of 3.84 km, L_y of 1.28 km and
321 L_z of 0.52 km as streamwise, lateral and vertical dimensions, respectively. Wind was driven
322 with a prescribed pressure gradient at $z > 250$ m, allowing the lower-altitude flow to attain a
323 constant momentum flux layer, which is characteristic for atmospheric boundary layer flows
324 (Stull, 2012). The magnitude of the pressure gradient was set sufficiently high to achieve very
325 high Reynolds number conditions, which ensures that the associated turbulence solution
326 attains a state that is independent of wind speed. That is, if the wind speed were further
327 increased, the turbulent structures and dynamics would remain statistically identical. This
328 Reynolds number independence allows one representative turbulent wind solution to be
329 freely scaled (especially upward) to represent other wind conditions. The simulation for the
330 (scalable) reference wind was initially run for one hour to allow the flow to reach a
331 statistically stationary state. The simulation was then continued for an additional hour during
332 which detailed wind velocity time series is collected every 3 s (at 1/3 Hz) across the entire
333 depth of the forest canopy from a 0.5-km² monitoring plane with 409 x 205 locations. This
334 time series contains a sample of 105.6×10^6 instantaneous wind events impacting the forest
335 canopy. As the main interest is on gusts whose duration is sufficient to cause further
336 displacements in the tree trunks, two consecutive wind events are averaged to yield a

337 conservative approximation for a 3-s gust. Thus, the time series contained approximately 50 x
338 10^6 gust events, which is considered a sufficiently large sample size to capture rare gust
339 events that impose the largest risk for trunk failure. The gust events causing the maximal
340 bending moments were searched by considering the forest canopy to contain trees with
341 uniform horizontal cross-sections (just for the sake of wind gust analysis). The bending
342 moment for each model tree was computed for all 3-s gust events and the maximum events
343 (time and location) were stored. The wind speed profile spanning across the tree height was
344 then obtained from this location and instance. The selected gust event provided the most
345 realistic estimation for the critical velocity distribution during a probable failure event.

346

347 In addition to the normal simulation named “Dense”, we performed a second simulation with
348 half of the sail area removed from all heights above ground (i.e. “Thinned”) and a third
349 simulation with trunks and branches remaining but leaves removed (i.e. “Leafless”).
350 However, it is important to note that these two secondary simulations violate the basis of our
351 modelling of trees evolved via thigmomorphogenesis to withstand a given above-canopy
352 wind speed by equal strain along the trunk, as a sudden thinning or defoliation would disturb
353 the balance to which trees have acclimated and trunks would therefore likely break from a
354 severely underbuilt segment before full bending is reached.

355

356 We computed the bending moments by adding moments from all segments and associated
357 branches and leaves above the segment in question (Fig. 3). We obtained the weights, i.e. the
358 vertical forces, by adding water contents of 0.79 for the trunk, 1.41 for the branches and 2.24
359 for leaves (Kantola and Makela, 2006; Kärkkäinen, 1985) to the dry masses (Kantola and
360 Mäkelä, 2004) and multiplying by the gravity constant (9.82 m s^{-2}). We did not take physical
361 contact between the trees into account.

362

363 The critical bending moment, i.e. the maximum bending moment that a cylindrical segment
364 can resist (m_r) is:

365

$$m_r = \frac{\sigma \pi d^3}{32} \quad (3)$$

366

367 where σ is modulus of rupture and d is the diameter of the segment (Ennos, 2012). The sum of
368 gravity- and wind-caused bending moments that cause this same m_r for the trunk segment is:

369

$$m_r = r^2 \sum m_u + \sum m_g, \quad (4)$$

370

371 where $\sum m_g$ is the sum of all gravity-caused bending moments of all the segments and
372 associated branches and leaves above, $\sum m_u$ is the sum of all wind-caused bending moments
373 from segments and associated branches and leaves above in a reference above-canopy mean
374 wind speed and r is the ratio of the maximum and reference (to compute $\sum m_u$) mean above-
375 canopy wind speeds based on the wind profile obtained from the PALM model. These steps
376 are shown as a flow chart in Fig. 4.

377

378 We then computed critical wind speeds that break the trunks in their weakest segments and
379 compared diameters of other segments to those needed to resist this wind. We did not “tune”
380 the approach or parameters to obtain a desirable fit. Below, we report the results from the
381 analysis planned before beginning analysing the data with the exception of exclusion of
382 recently thinned plots.

383

384

385 **Results**

386

387 Most of the sail area of the five felled trees is caused by leaves and is located, once the trees
388 are storm-bent, at a height of 15–21 m (Fig 5a). When the surrounding trees are added, the
389 layer of dense sail area thickens, mainly upward (Fig 5b), but is still surprisingly thin for a
390 tree species having an unusually long crown. The lack of thinnings in the studied stand has
391 probably resulted in unusually small crown ratios and thin trunks enabling considerable
392 bending, both of which thin the layer of dense sail area in a storm-bent stand.

393

394 The gust wind speeds are weak below 8 m, and increase roughly linearly upwards through the
395 main sail area in Dense and Thinned stands (Fig. 5c). However gust wind is significant down
396 to the ground in the Leafless stand (Fig. 5c).

397

398 The weight of the branchless lower parts of the trunks of all five felled trees is important, but
399 they cause bending moments only to the lower segments of the trunk. These moments are
400 small, as the segments are nearly vertically aligned (Fig. 6). The weights from the upper
401 segments and associated branches and leaves that produce potentially more significant
402 bending moments are roughly evenly divided by those caused by the trunk, branches and
403 leaves (Fig. 6). The comparison between trees illustrates how trees with larger $d_{1.3}$ (Tree4 and
404 Tree5) have correspondingly heavier crowns but the differences are small. The differences
405 between the five trees are much more significant when the horizontal vectors caused by wind
406 are examined (Fig. 6). The smallest trees experience much greater forces caused by gravity
407 than wind, whereas both forces are of the same magnitude in the crowns of the largest trees.
408 However, the wind-caused forces act higher up along the trunk and their direction also causes
409 greater strengthening requirements for the lower trunk. Because the top of storm-bent Tree1

410 is only at a height of 16.1 m, it is well protected by more rigid taller trees (Fig. 6).
411 Interestingly, because the shorter trees bend more, the horizontal displacement caused by
412 wind is approximately the same for all five trees, ranging from 12.7 m (Tree5) to 14.3
413 (Tree3).

414

415 Gravity from all segments and associated branches and leaves above the height at which the
416 focus is 18–27% of the bending moment that breaks a tree at a height of 1.3 m (Fig. 7). This
417 proportion increases upwards to a height of 12–15 m with the lowest branches and then
418 decreases down to a rounded 0% for the tops of the trees. However, as bark is included in the
419 used d and the wood characteristics are unusual for the topmost segments, the estimated
420 proportion is likely to be a severe underestimation. Nevertheless, the proportion of gravity
421 relative to the critical bending moment clearly decreases upwards in the canopy.

422

423 Fig. 8 demonstrates the dimensions of the five felled trees without wind and in addition to the
424 measured diameters, the diameters needed to resist an above-canopy mean wind of 10.2 m s^{-1} ,
425 which is the speed that is at the limit of breaking Tree4. This can be seen from the dotted red
426 line contacting the solid black line at a height of 13.9 m. Tree3 and Tree5 are able to resist
427 similar mean above-canopy wind speeds (12.7 m s^{-1} and 11.3 m s^{-1}), and therefore the
428 modelled taper is similar to the measured taper (Fig. 8). However, for Tree2 and especially
429 Tree1, a significantly thinner trunk would be sufficient to withstand the simulated gust with
430 an above-canopy mean wind of 10.2 m s^{-1} . The simulated gust increases wind speeds
431 considerably, reaching 34.2 m s^{-1} above-canopy (height of 29.25 m) and decreasing
432 downwards as shown in Fig. 5c, with a speed of 25.9 m s^{-1} in the upper part (height of 21.75
433 m) of the storm-bent main canopy and 5.6 m s^{-1} in the lower part (height of 12.75 m).

434

435 The above-canopy mean wind speed in the thinned stand is surprisingly similar to that above
436 the dense stand, and rounds to the same 10.2 m s^{-1} in the equivalent meteorological situation
437 and is slightly weaker in the strongest gust at 33.2 m s^{-1} . However, the winds are stronger
438 within the canopy, and for all except Tree1, greater diameters would have been needed to
439 resist breaking (Fig. 8), indicating that thinnings increase the risk of stem breakage.

440

441 The wind simulation for a leafless stand resulted in an above-canopy mean wind speed of
442 14.6 m s^{-1} (gust 36.3 m s^{-1}) in the same meteorological situation as discussed above and the
443 wind penetrated the stand with much more force (Fig. 5c). A significantly smaller diameter
444 for all trees and along all heights would be sufficient in this situation (Fig. 8), as sail areas of
445 the trees decreased.

446

447

448 **Discussion**

449

450 We developed a novel approach to model bending moments of storm-bent trees caused by
451 wind and gravity and applied this to an unthinned middle-aged *Picea* stand originated from
452 planted seedlings. We focused on winds that break the weakest segments and observed a
453 close match of modelled and the actual diameters along other segments their trunks for most
454 of the trees (Fig. 8). Therefore, we may conclude that these bending moments are probably
455 important in determining trunk diameter and shape, but we are unable to compare importance
456 of alternative determinants of tree size such as sap transport. The relatively small contribution
457 of a tree's own mass (Fig. 7) indicates that, if to simplify only gravity or wind can be
458 included in the modelling, wind would probably be a better choice, even in a dense unthinned
459 stand (e.g. Larjavaara, 2010) with small sail areas relative to fresh masses. The studied trees

460 where probably much closer to elastic buckling than plants in the dataset of Niklas (1994)
461 and may be close to bending even in windless conditions due to the extra weight of snow.
462
463 Our simulated winds may be compared to those within (at a height of 9 m) and above (at a
464 height of 23 m) a 16-m tall *Pinus sylvestris* stand during a summer microburst that toppled
465 over trees approximately 300 m from the wind measurements (Järvi et al., 2007). The
466 microburst caused one-minute mean wind speeds of ca. 14 m s⁻¹ above and 5 m s⁻¹ within the
467 canopy. The above-canopy speed is close to the winds that our five trees can resist, with the
468 exception of Tree1 (Fig. 8). Furthermore, the wind speed within the relatively sparse *Pinus*
469 canopy corresponds to values that may have been expected based on our wind profiles (Fig.
470 5c). However, the variation in windspeed measured by Järvi et al. (2007) was much lower, as
471 their “instantaneous” above-canopy wind speeds peaked at only just above 20 m s⁻¹. This may
472 indicate that our biomechanical computations overestimated the resistance of trees to bending
473 forces. However, as the damaged *Pinus* trees were located some distance away from the
474 anemometers, it is likely they experienced much stronger wind speeds than recorded at the
475 specific location of the sensors.

476

477 Our objectives were to understand more about trunk taper based on wind and the risks that
478 trees potentially take, whereas the majority of research linking taper, wind and risks inversely
479 attempt to estimate risks from taper and winds (Gardiner et al., 2008). The demand for advice
480 from forest managers is substantial both in plantations (Gardiner et al., 2016) and urban
481 setting (Sæbø et al., 2003), and advances have been impressive (Gardiner et al., 2019).
482 However, a pessimist may argue that scientists will never be “wiser” than an acclimated tree
483 in “understanding” the local wind profile and risks caused by extreme gusts. From an
484 evolutionary perspective, trees balance between having their trunks breaking in a storm and

485 overinvesting in trunk tissue and being overtopped by their neighbours growing faster. A
486 winning strategy optimally balancing between the deadly “ditches” on both sides depends on
487 the position of the other ditch. Hence, in a situation with fierce competition and high
488 likelihood of being overtopped by neighbours, such as in middle-aged dense plantations, the
489 risk on trunk breakage in a storm is increased. Therefore, the most fruitful theoretical (not
490 just statistical and descriptive) way to estimate the risk of trunk breakage may be based on
491 competition for height from an evolutionary perspective. Physical modelling, such as that
492 used in this article but inversely, is more promising for trees in situations have not acclimated
493 to, e.g. after their neighbours have been harvested (e.g. Peltola et al., 1999).

494

495 In our simulation of the strongest gust, it is remarkable how a *Picea abies* monoculture,
496 characterised by long, conical, and slender crowns, forms a relatively thin layer of dense sail
497 area of sail area at approximately 18 m above ground during a gust. To support a larger leaf
498 mass, a tree needs to build a thicker trunk to resist the wind drag and gravity acting on this
499 additional mass. Even without additional height when unbent, the additional diameter reduces
500 bending and the storm-bent height increases. Because trees with thicker trunks are normally
501 also taller, they have greater wind drag caused by bending moments because of greater sail
502 area and this area being located in greater winds because of greater unbent height but also
503 reduced bending. The thicker trees in a stand are responsible for blocking wind and
504 protecting the smaller “biomechanical free-riders”. This mechanism operates as a balancing
505 force, i.e. negative feedback, in stand development, thanks to which height growth of shorter
506 trees is boosted relative to the tall ones.

507

508 Tree1 is much thicker and Tree2 is to some extent thicker than they need to be to resist the
509 modelled gust. Their positions in the canopy may have weakened rapidly, leaving their

510 thicker trunks as a legacy of a time when they needed strength for a larger leaf area, but
511 biomechanically they would not then need new diameter growth. Also the transport-focused
512 perspective offers an alternative explanation. When trees become suppressed in the canopy,
513 they rapidly lose their lower branches and their crown length grows more slowly than their
514 height, reducing their crown ratio. This change in growth pattern may be regarded as an
515 evolutionary response to competition for light (e.g. Mäkelä, 1985). In this process, active
516 wood, i.e. sapwood, related to the receding branches loses its connection to the foliage and
517 gradually turns into inactive heartwood. Empirical evidence and eco-evolutionary balance
518 theories suggest that active wood area and foliage area are in balance with each other (Chiba
519 et al., 1988; Mäkelä and Valentine, 2006; Shinozaki et al., 1964). Losing the active wood
520 related to the receding branches therefore creates a need for new diameter growth to build
521 new sapwood, as the existing inactive wood can no longer be used for water transport. If we
522 assume that all these selective pressures, related to biomechanics, water transport, and
523 competition for light, are present in the tree population, then our results suggest that
524 biomechanics dominate trunk dimensions of dominant trees (see also Mäkelä and Valentine,
525 2006), while with suppressed trees the balance has possibly shifted from biomechanics
526 towards sap transport. Another reason for our result that smaller trees have larger diameters
527 than apparently necessary may be that our wind model severely overestimates the steepness
528 of the vertical wind profile. It is also possible that suppressed trees occasionally experience
529 unusually strong gusts that penetrate the canopy but which was not our “strongest gust” due
530 to our sampling, and are therefore seemingly overbuilt. Supressed trees could also be
531 prepared for surviving the gust that break their supressors. These questions could be studied
532 by analysing how tree size influences mortality in storms.

533

534 The tops of all five trees appear overbuilt. We can try to understand this by comparing small
535 trees of the same height that may initially seem to have nearly identical biomechanical
536 constraints. Coincidentally, both small *Picea* trees and residue treetops have commonly been
537 used as Christmas trees in Finland and are easy to differentiate even from a distance. Treetops
538 need to resist much stronger winds but can streamline easier, as their bases are tilted thanks to
539 the bending lower trunk. Probably most importantly, treetops cannot rely on the “shrub
540 strategy” of bending all the way to the ground to remain unharmed (Larjavaara, 2015). This
541 makes small trees resistant to the strongest winds and heaviest snowloads, as they can bounce
542 back after a gust has passed or the snow has melted. Treetops however, cannot rely on ground
543 support during gusts, but this is probably not a problem for the well-streamlined tops of *Picea*
544 *abies* (Fig. 6). Snow weight, which may be significant in the region especially when
545 temperatures are close to freezing or when direct condensation occurs on trees, is a possible
546 reason for the seemingly overbuilt tops in our dataset (Peltola et al., 1999).

547

548 We focused on an unthinned boreal monoculture, i.e. nearly the simplest stand imaginable –
549 only treetops could potentially have been easier to understand in an ice-free climate. We
550 nevertheless had to make many simplifying assumptions. The risk of resonating with the
551 wind is a serious concern in designing structures, such as bridges, and the risk of trees
552 swaying with a pulsing wind has often been the focus of trunk breakage literature (Niklas and
553 Spatz, 2012). However, air flow modelling does not seem to create such winds (Gardiner et
554 al., 2019) and is rarely seen in dozens of videos found on the Internet that depict uprooting or
555 trunk breakage (ML personal observation), but scientific evidence is needed (Moore et al.,
556 2018). Similarly, torsional forces have attracted some attention (Skatter and Kucera, 2000),
557 but it is likely that strengthening the trunks to resist twisting could be achieved easier by
558 adjusting wood characteristics without increasing trunk diameters. Uprooting possibly being

559 more common than trunk breakage is one argument against the biomechanical modelling of
560 trunks, but this does not rule out the importance of trunk dimensions on trunk failure. In their
561 evolutionary history, trees have probably balanced the risks of uprooting and trunk breakage
562 depending on the level and variability of risks and on the cost of strengthening them. Our
563 assumptions that the same level of streamlining occurs at all heights (Online Resource 1) and
564 invariable, modulus of rupture (σ) and modulus of elasticity (E), may be far from realistic but
565 probably do not interfere significantly with our comparison between trees and along the trunk
566 of one tree, except perhaps in the tops which may in reality be more flexible due to juvenile
567 wood and therefore e.g. the relative importance of gravity would be underestimated (Fig. 7).
568 Choosing the value for drag coefficient (C_d) was rather arbitrary as always. Furthermore, we
569 did not attempt to include physical contact with neighbours influencing the bending forces.
570 Such canopy contacts may be harmful, as tree tissue may be damaged, but on the other hand
571 they may save a tree that is supported by a neighbour in extreme winds.

572

573 Our greatest concern relates to dealing with streamlining and the homogeneousness of the sail
574 area. We assumed 50% streamlining for branches and none for leaves (Online Resource 1).
575 This is probably an underestimation (Peltola et al., 1999), but perhaps surprisingly it does not
576 strongly influence this kind of analysis related to trunk diameters, as despite streamlining
577 reducing wind drag caused by a given wind speed, it increases wind speeds within the stand.
578 For example, the Thinned simulation with half of the sail area removed corresponds to the
579 Dense simulation with streamlining reducing the projected area to half its original size. This
580 allows us to estimate the sensitivity of our results to assumptions on streamlining.
581 Interestingly, the wind-caused bending moments were larger for two of our five trees, with
582 50 % stronger streamlining, while they were smaller for three trees. This indicates that our
583 results are not very sensitive to streamlining, as the increasing wind speed due to streamlining

584 compensates for the reduced sail area. Similarly, the spatial grouping of sail area is probably
585 important and drastically influences both winds and the drags that they cause. However,
586 again it is possible that reduced winds for a given wind speed cause greater within-canopy
587 winds thanks to the clustering of sail area, and their impacts may roughly even out as with the
588 cause of streamlining.

589

590 Our approach could be utilized in several applications. Evolutionary simulations could
591 optimize trunk dimensions by considering the benefits of being a biomechanical free-rider
592 and relying on larger neighbour trees to withstand wind, but potentially face local extinction
593 if all canopy species or individuals take excessive risks and rely on trunks of others not
594 breaking. Other mechanistic modelling approaches (Kalliokoski et al., 2016), which are
595 potentially especially valuable when optimizing forest management in changed conditions,
596 may also benefit from incorporation of wind- and gravity-driven trunk diameter modelling,
597 e.g. by increasing detail in the direction pointed by Eloy et al. (2017).

598

599 **Availability of data and materials**

600 The dataset will be made available in a location specified later.

601

602 **Conflict of interest**

603 The authors declare that they have no conflict of interest

604

605 **Funding**

606 ML acknowledges Peking University for funding.

607

608 **Author's contributions**

609 ML and AM developed the research idea, AK designed and implemented the data collection
610 procedure supervised by AM, MA performed the wind simulations and wrote the first draft of
611 its description, ML performed the other analyses, prepared the figures and wrote the first
612 draft of the other sections, and all authors participated in producing the final version of the
613 manuscript.

614

615 **Acknowledgements**

616 We thank Tapio Linkosalo for discussions in the early stages of the research process and
617 Stella Thompson for English language editing.

618 **References**

619

- 620 Anderson-Teixeira KJ, Miller AD, Mohan JE, Hudiburg TW, Duval BD, DeLucia EH (2013) Altered
621 dynamics of forest recovery under a changing climate. *Global Change Biology* 19: 2001-2021
- 622 Badel E, Ewers FW, Cochard H, Telewski FWJFiPS (2015) Acclimation of mechanical and hydraulic
623 functions in trees: impact of the thigmomorphogenetic process 6: 266
- 624 Bianchi S, Huuskonen S, Siipilehto J, Hynynen J (2020) Differences in tree growth of Norway spruce
625 under rotation forestry and continuous cover forestry. *Forest Ecology and Management* 458
- 626 Bonnesoeur V, Constant T, Moulia B, Fournier M (2016) Forest trees filter chronic wind-signals to
627 acclimate to high winds. *New Phytol.* 210: 850-860
- 628 Brüchert F, Gardiner B (2006) The effect of wind exposure on the tree aerial architecture and
629 biomechanics of Sitka spruce (*Picea sitchensis*, Pinaceae). *American journal of botany* 93: 1512-1521
- 630 Butler DW, Gleason SM, Davidson I, Onoda Y, Westoby M (2012) Safety and streamlining of woody
631 shoots in wind: an empirical study across 39 species in tropical Australia. *New Phytol.* 193: 137-149
- 632 Cajander AK (1949) Forest types and their significance. *Acta Forestalia Fennica* 56: 1-72
- 633 Canadell J, López-Soria L (1998) Lignotuber reserves support regrowth following clipping of two
634 Mediterranean shrubs. *Functional Ecology* 12: 31-38
- 635 Caudullo G, Tinner W, de Rigo D (2016) *Picea abies* in Europe: distribution, habitat, usage and
636 threats. In: San-Miguel-Ayanz J, de Rigo D, Caudullo G, Houston Durrant T, Mauri A (eds) *European*
637 *Atlas of Forest Tree Species*
- 638 Chapotin SM, Razanameharizaka JH, Holbrook NM (2006) Baobab trees (*Adansonia*) in Madagascar
639 use stored water to flush new leaves but not to support stomatal opening before the rainy season.
640 *New Phytol.* 169: 549-559
- 641 Chave J, Coomes D, Jansen S, Lewis SL, Swenson NG, Zanne AE (2009) Towards a worldwide wood
642 economics spectrum. *Ecology Letters* 12: 351-366
- 643 Chave J, Rejou-Mechain M, Burquez A, Chidumayo E, Colgan MS, Delitti WBC, Duque A, Eid T,
644 Fearnside PM, Goodman RC, Henry M, Martinez-Yrizar A, Mugasha WA, Muller-Landau HC,
645 Mencuccini M, Nelson BW, Ngomanda A, Nogueira EM, Ortiz-Malavassi E, Pelissier R, Ploton P, Ryan
646 CM, Saldarriaga JG, Vieilledent G (2014) Improved allometric models to estimate the aboveground
647 biomass of tropical trees. *Global Change Biology* 20: 3177-3190
- 648 Chiba Y, Fujimori T, Kiyono Y (1988) Another interpretation of the profile diagram and its availability
649 with consideration of the growth process of forest trees. *Journal of the Japanese Forestry Society* 70:
650 245-254
- 651 Collalti A, Tjoelker MG, Hoch G, Mäkelä A, Guidolotti G, Heskell M, Petit G, Ryan MG, Battipaglia G,
652 Matteucci G (2019) Plant respiration: controlled by photosynthesis or biomass? *Global Change*
653 *Biology*
- 654 Eloy C, Fournier M, Lacoite A, Moulia B (2017) Wind loads and competition for light sculpt trees
655 into self-similar structures. *Nat. Commun.* 8: 1014
- 656 Ennos AR (2012) *Solid biomechanics*. Princeton University Press
- 657 Gardiner B, Achim A, Nicoll B, Ruel J-C (2019) Understanding the interactions between wind and
658 trees: an introduction to the IUFRO 8th Wind and Trees Conference (2017). *Forestry: An*
659 *International Journal of Forest Research* 92: 375-380
- 660 Gardiner B, Berry P, Moulia B (2016) Wind impacts on plant growth, mechanics and damage. *Plant*
661 *Science* 245: 94-118
- 662 Gardiner B, Byrne K, Hale S, Kamimura K, Mitchell SJ, Peltola H, Ruel J-C (2008) A review of
663 mechanistic modelling of wind damage risk to forests. *Forestry: An International Journal of Forest*
664 *Research* 81: 447-463
- 665 Ichihashi R, Tateno M (2015) Biomass allocation and long-term growth patterns of temperate lianas
666 in comparison with trees. *New Phytol.* 207: 604-612

667 Jackson T, Shenkin A, Wellpott A, Calders K, Origo N, Disney M, Burt A, Raunonen P, Gardiner B,
668 Herold M (2019) Finite element analysis of trees in the wind based on terrestrial laser scanning data.
669 *Agricultural forest meteorology* 265: 137-144

670 Järvi L, Punkka A-J, Schultz DM, Petäjä T, Hohti H, Rinne J, Pohja T, Kulmala M, Hari P, Vesala T (2007)
671 Micrometeorological observations of a microburst in southern Finland. *Atmospheric Boundary*
672 *Layers*. Springer, pp 187-203

673 Kalliokoski T, Mäkinen H, Linkosalo T, Mäkelä A (2016) Evaluation of stand-level hybrid PipeQual
674 model with permanent sample plot data of Norway spruce. *Canadian Journal of Forest Research* 47:
675 234-245

676 Kantola A, Makela A (2006) Development of biomass proportions in Norway spruce (*Picea abies* L.
677 Karst.). *Trees-Structure and Function* 20: 111-121

678 Kantola A, Mäkelä A (2004) Crown development in Norway spruce [*Picea abies* (L.) Karst.]. *Trees*
679 *Structure & Functioning* 18: 408-421

680 Kärkkäinen M (1985) Puutiede. Sällisen kustannus

681 Katul G (1998) An investigation of higher-order closure models for a forested canopy. *Boundary-*
682 *Layer Meteorology* 89: 47-74

683 Klein T, Randin C, Korner C (2015) Water availability predicts forest canopy height at the global scale.
684 *Ecology Letters* 18: 1311-1320

685 Koch GW, Sillett SC, Jennings GM, Davis SD (2004) The limits to tree height. *Nature* 428: 851-854

686 Kuuluvainen T, Aakala T (2011) Natural forest dynamics in boreal Fennoscandia: a review and
687 classification. *Silva Fennica* 45: 823-841

688 Larjavaara M (2010) Maintenance cost, toppling risk and size of trees in a self-thinning stand. *Journal*
689 *of Theoretical Biology* 265: 63-67

690 Larjavaara M (2015) Trees and shrubs differ biomechanically. *Trends Ecol. Evol.* 30: 499-500

691 Larjavaara M (2021) What would a tree say about its size? *Frontiers in Ecology and Evolution* 8

692 Larjavaara M, Muller-Landau HC (2012) Still rethinking the value of high wood density. *American*
693 *Journal of Botany* 99: 165-168

694 Mäkelä A (1985) Differential games in evolutionary theory: height growth strategies of trees.
695 *Theoretical Population Biology* 27: 239-267

696 Mäkelä A (2002) Derivation of stem taper from the pipe theory in a carbon balance framework. *Tree*
697 *Physiology* 22: 891-905

698 Mäkelä A, Valentine HT (2006) Crown ratio influences allometric scaling in trees. *Ecology Letters* 87:
699 2967-2972

700 Maronga B, Gryscha M, Heinze R, Hoffmann F, Kanani-Sühring F, Keck M, Ketelsen K, Letzel MO,
701 Sühring M, Raasch S (2015) The Parallelized Large-Eddy Simulation Model (PALM) version 4.0 for
702 atmospheric and oceanic flows: model formulation, recent developments, and future perspectives.
703 *Geoscientific Model Development Discussions* 8

704 Mattheck C (2000) Comments on "Wind-induced stresses in cherry trees: evidence against the
705 hypothesis of constant stress levels" by KJ Niklas, H.-C. Spatz, *Trees* (2000) 14: 230-237. *Trees*
706 *Structure & Functioning* 15

707 Mattheck GC (2012) *Trees: the mechanical design*. Springer Science & Business Media

708 McMahon T (1973) Size and shape in biology. *Science* 179: 1201-1204

709 Metzger K (1893) Der Wind als maßgebender Faktor für das Wachstum der Bäume. *Mündener*
710 *Forstliche Hefte* 5: 35-86

711 Moore J, Gardiner B, Sellier D (2018) Tree mechanics and wind loading. *Plant biomechanics*.
712 Springer, pp 79-106

713 Morgan J, Cannell MG (1994) Shape of tree stems—a re-examination of the uniform stress
714 hypothesis. *Tree physiology* 14: 49-62

715 Niez B, Dlouha J, Moulia B, Badel EJT (2019) Water-stressed or not, the mechanical acclimation is a
716 priority requirement for trees 33: 279-291

717 Niklas KJ (1994) INTERSPECIFIC ALLOMETRIES OF CRITICAL BUCKLING HEIGHT AND ACTUAL PLANT
718 HEIGHT. *American Journal of Botany* 81: 1275-1279

719 Niklas KJ, Spatz H-C (2000) Wind-induced stresses in cherry trees: evidence against the hypothesis of
720 constant stress levels. *Trees Structure & Functioning* 14: 230-237

721 Niklas KJ, Spatz HC (2012) *Plant Physics*. University of Chicago Press

722 Patrut A, Mayne DH, von Reden KF, Lowy DA, Van Pelt R, McNichol AP, Roberts ML, Margineanu D
723 (2010) Fire history of a giant African baobab evinced by radiocarbon dating. *Radiocarbon* 52: 717-
724 726

725 Peltola A (2014) *Metsätilastollinen vuosikirja 2014*

726 Peltola H, Kellomäki S, Hassinen A, Granander M (2000) Mechanical stability of Scots pine, Norway
727 spruce and birch: an analysis of tree-pulling experiments in Finland. *Forest Ecology And*
728 *Management* 135: 143-153

729 Peltola H, Kellomäki S, Väisänen H, Ikonen V-P (1999) A mechanistic model for assessing the risk of
730 wind and snow damage to single trees and stands of Scots pine, Norway spruce, and birch. *Canadian*
731 *Journal of Forest Research* 29: 647-661

732 Pruyt ML, Ewers III BJ, Telewski FWJTP (2000) Thigmomorphogenesis: changes in the morphology
733 and mechanical properties of two *Populus* hybrids in response to mechanical perturbation 20: 535-
734 540

735 Ryan MG, Yoder BJ (1997) Hydraulic limits to tree height and tree growth. *Bioscience* 47: 235-242

736 Sæbø A, Benedikz T, Randrup TBJUF, Greening U (2003) Selection of trees for urban forestry in the
737 Nordic countries 2: 101-114

738 Schiestl-Aalto P, Kulmala L, Mäkinen H, Nikinmaa E, Mäkelä A (2015) CASSIA—a dynamic model for
739 predicting intra-annual sink demand and interannual growth variation in Scots pine. *New Phytol.*
740 206: 647-659

741 Scholz FG, Phillips NG, Bucci SJ, Meinzer FC, Goldstein G (2011) Hydraulic capacitance: biophysics
742 and functional significance of internal water sources in relation to tree size. Size- and age-related
743 changes in tree structure and function. Springer, pp 341-361

744 Shinozaki K, Yoda K, Hozumi K, Kira T (1964) A quantitative analysis on plant form - The pipe model
745 theory. I - Basic analyses. *Japanese Journal of Ecology* 14: 97-105

746 Skatter S, Kucera B (2000) Tree breakage from torsional wind loading due to crown asymmetry.
747 *Forest Ecology Management* 135: 97-103

748 Spatz H-C, Bruechert F (2000) Basic biomechanics of self-supporting plants: wind loads and
749 gravitational loads on a Norway spruce tree. *Forest Ecology Management* 135: 33-44

750 Stull RB (2012) *An introduction to boundary layer meteorology*. Springer Science & Business Media

751 Telewski FW (2016) Flexure wood: mechanical stress induced secondary xylem formation.
752 *Secondary Xylem Biology*. Elsevier, pp 73-91

753 Van Pelt R, Sillett SC, Kruse WA, Freund JA, Kramer RD (2016) Emergent crowns and light-use
754 complementarity lead to global maximum biomass and leaf area in *Sequoia sempervirens* forests.
755 *Forest Ecology Management* 375: 279-308

756 West GB, Brown JH, Enquist BJ (1999) A general model for the structure and allometry of plant
757 vascular systems. *Nature* 400: 664-667

758 Wicker LJ, Skamarock WC (2002) Time-splitting methods for elastic models using forward time
759 schemes. *Monthly weather review* 130: 2088-2097

760 Woodruff DR (2013) The impacts of water stress on phloem transport in Douglas-fir trees. *Tree*
761 *physiology* 34: 5-14

762 Yoda K, Kira T, Ogawa H, Hozumi K (1963) Self-thinning in overcrowded pure stands under cultivated
763 and natural conditions. *Journal of Biology, Osaka City University* 14: 107-129

764

765

766

767 **Figure captions**

768

769 Figure 1. Storm-bent height of the five felled trees plotted against $d_{1.3}$ and a fitted linear
770 regression model. R^2 is the coefficient of determination.

771

772 Figure 2. Storm-bent height of the five felled trees multiplied by their sail area (projected
773 area of trunk, branches and leaves) plotted against the cube of $d_{1.3}$ and a fitter linear
774 regression model. R^2 is the coefficient of determination.

775

776 Figure 3. An example of how we computed the bending moments from the forces caused by
777 gravity and wind blowing from left to right. The “dashed” line represents storm-bent Tree3
778 with 18 uneven segments visible out of its 35 segments. The vectors show how we
779 computed the moment caused by the 11th topmost segment to the 3rd lowest segment
780 (both of which are highlighted with a thicker red line).

781

782 Figure 4. Calculation of bending moments on segments.

783

784 Figure 5. Sail area and winds in a gust at various heights in the canopy and just above.

785

786 Figure 6. The five felled trees shown as storm-bent. The number of the poorly visible
787 topmost segments that have bent to horizontal ranges from 4 (Tree5) to 11 (Tree2). The
788 green, red and blue horizontal lines represent force vectors caused by wind in the dense
789 simulation on each segment, with the colour indicating whether the drag is caused by the
790 trunk, branches or leaves. The vertical lines represent forces caused by gravity. The length of

791 vertical vectors from the lowest segments is not shown. The bottom end of a vector is -5.7
792 from the lowest segment of Tree5 with the same scale below the 0-level of the Y-axis as
793 above.

794

795 Figure 7. The relative importance of the bending moment caused by gravity acting on
796 segments and associated branches and leaves above the segment in question.

797

798 Figure 8. The dimensions of five felled tree trunks (solid black) and dimensions sufficient to
799 withstand wind and gravity (dotted and dashed lines) in a meteorological situation that
800 causes a mean wind above the canopy of the dense stand (w) of 10.2 m s^{-1} , which is the
801 critical speed that nearly breaks Tree4. The heights on vertical axis and diameters on the
802 horizontal axis are not proportional. Diameters at a height of 1.3 m are given in the bottom.
803 The critical above-canopy wind speed for the dense stand is indicated inside the trunks. The
804 lowest living branches were at heights of 11.2–14.5 m.

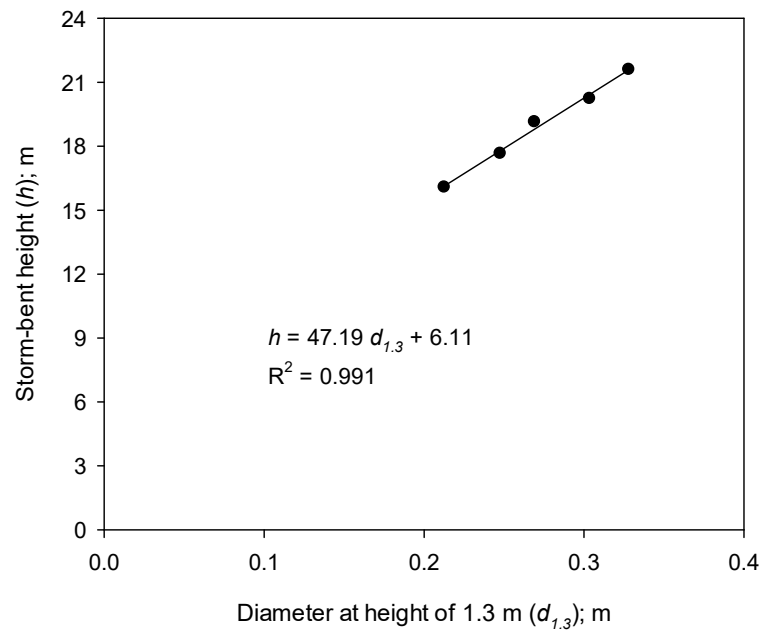


Figure 1. Storm-bent height of the five felled trees plotted against $d_{1.3}$ and a fitted linear regression model. R^2 is the coefficient of determination.

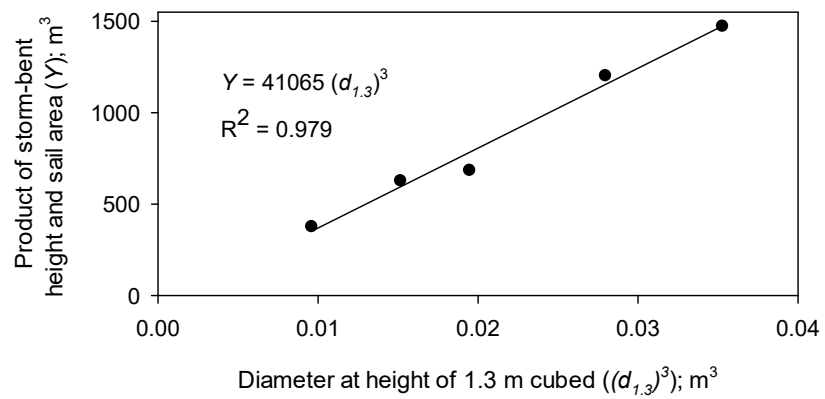


Figure 2. Storm-bent height of the five felled trees multiplied by their sail area (projected area of trunk, branches and leaves) plotted against the cube of $d_{1.3}$ and a fitter linear regression model. R^2 is the coefficient of determination.

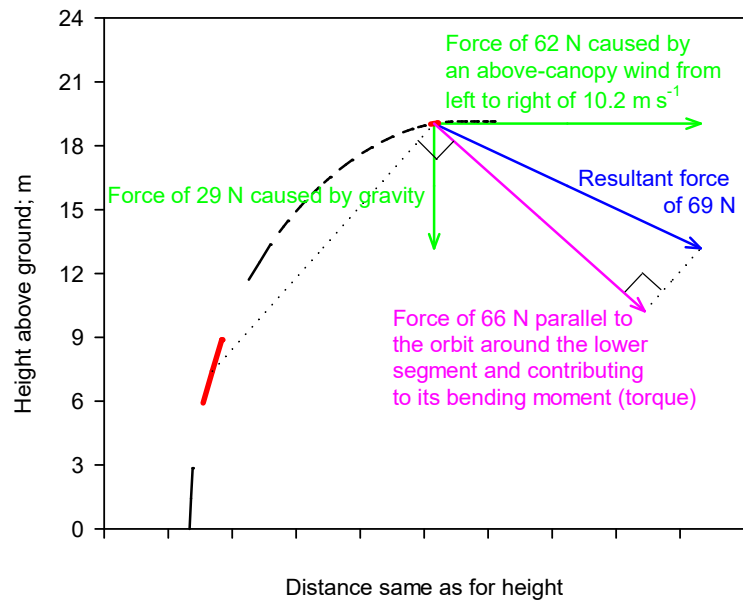


Figure 3. An example of how we computed the bending moments from the forces caused by gravity and wind blowing from left to right. The “dashed” line represents storm-bent Tree3 with 18 uneven segments visible out of its 35 segments. The vectors show how we computed the moment caused by the 11th topmost segment to the 3rd lowest segment (both of which are highlighted with a thicker red line).

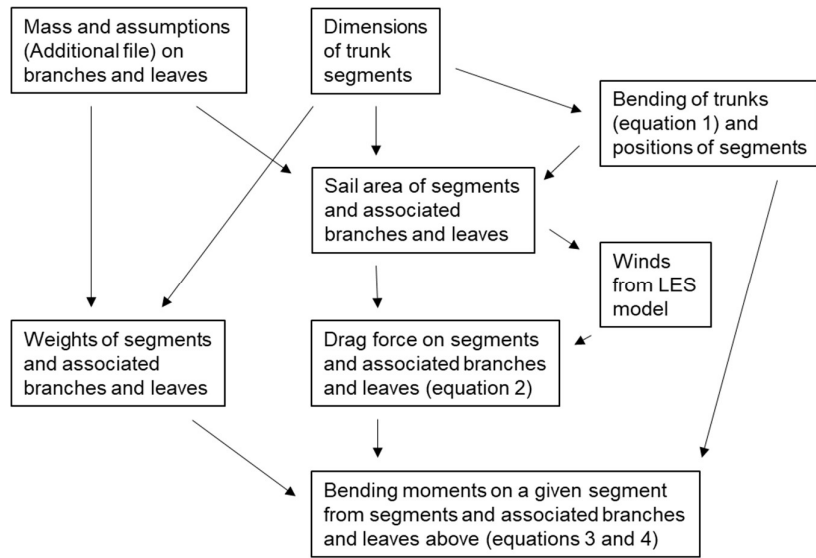


Figure 4. Calculation of bending moments on segments.

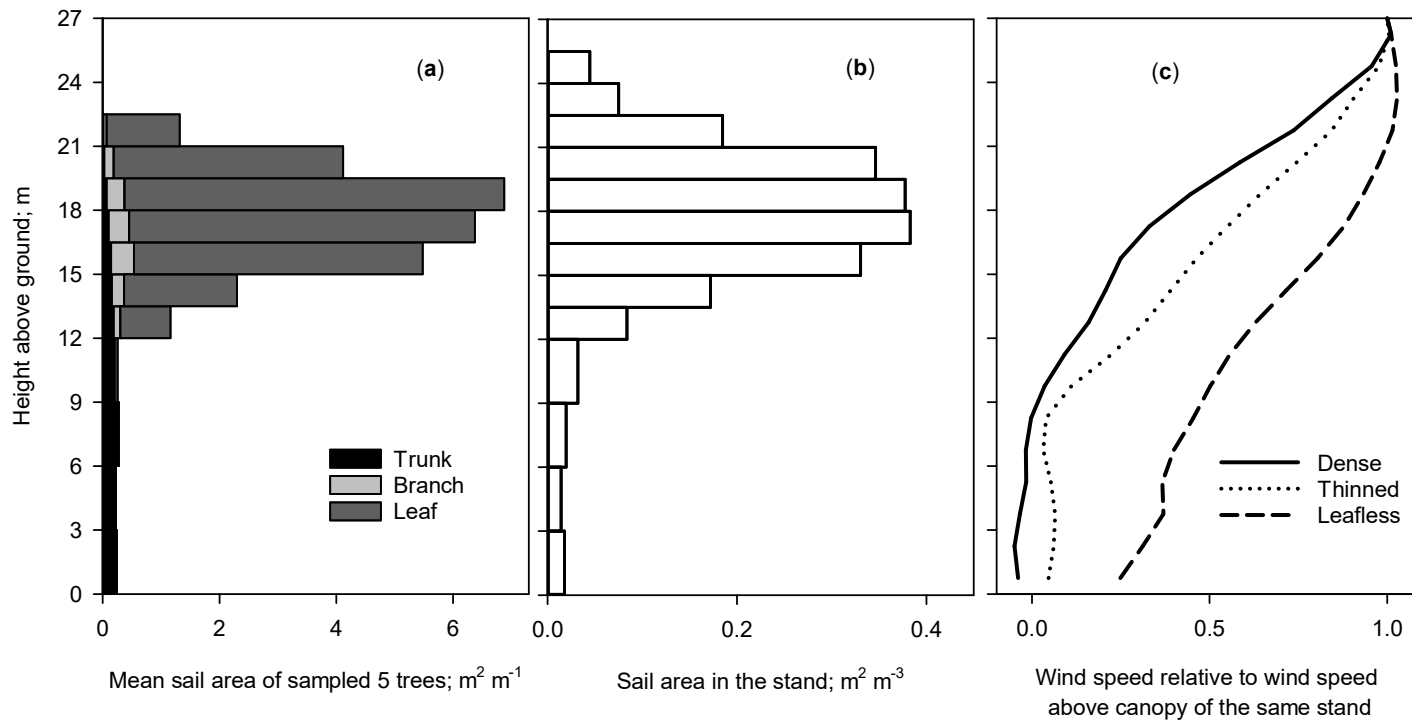


Figure 5. Sail area and winds in a gust at various heights in the canopy and just above.

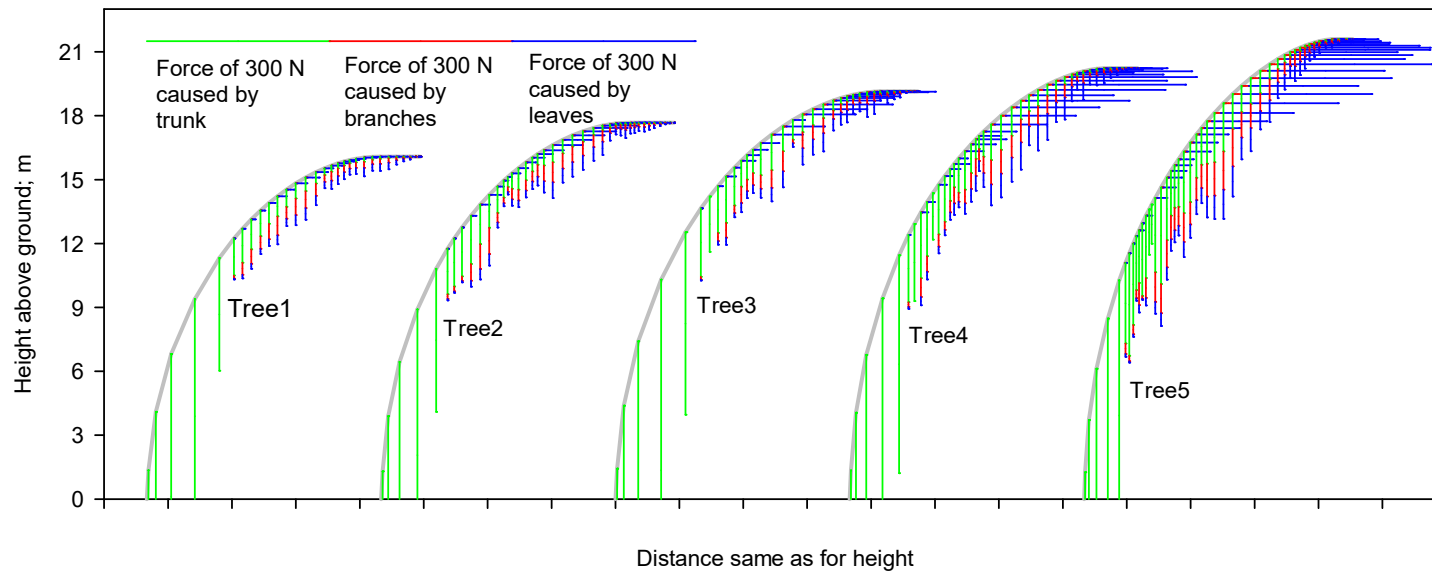


Figure 6. The five felled trees shown as storm-bent. The number of the poorly visible topmost segments that have bent to horizontal ranges from 4 (Tree5) to 11 (Tree2). The green, red and blue horizontal lines represent force vectors caused by wind in the dense simulation on each segment, with the colour indicating whether the drag is caused by the trunk, branches or leaves. The vertical lines represent forces caused by gravity. The length of vertical vectors from the lowest segments is not shown. The bottom end of a vector is -5.7 from the lowest segment of Tree5 with the same scale below the 0-level of the Y-axis as above.

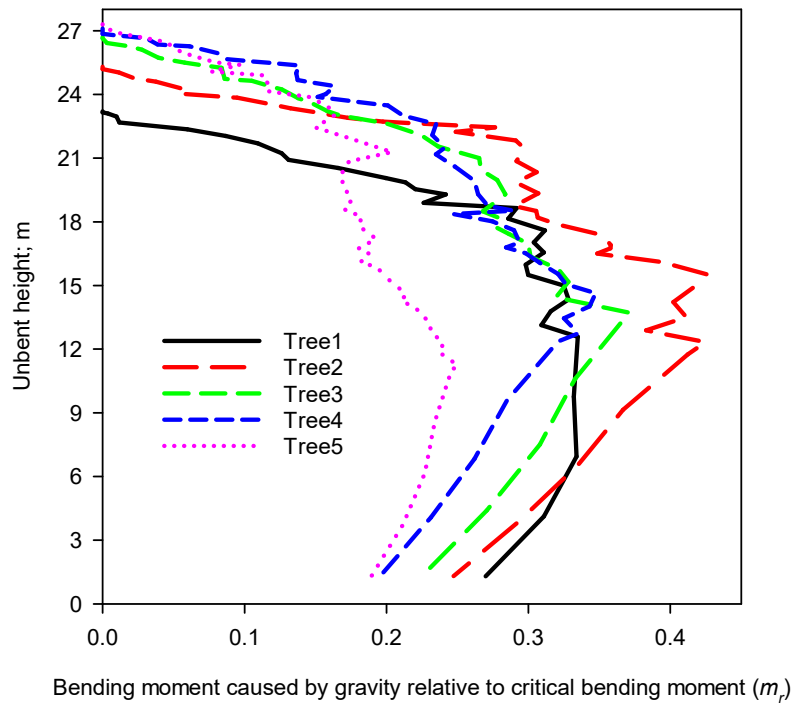


Figure 7. The relative importance of the bending moment caused by gravity acting on segments above the segment in question.

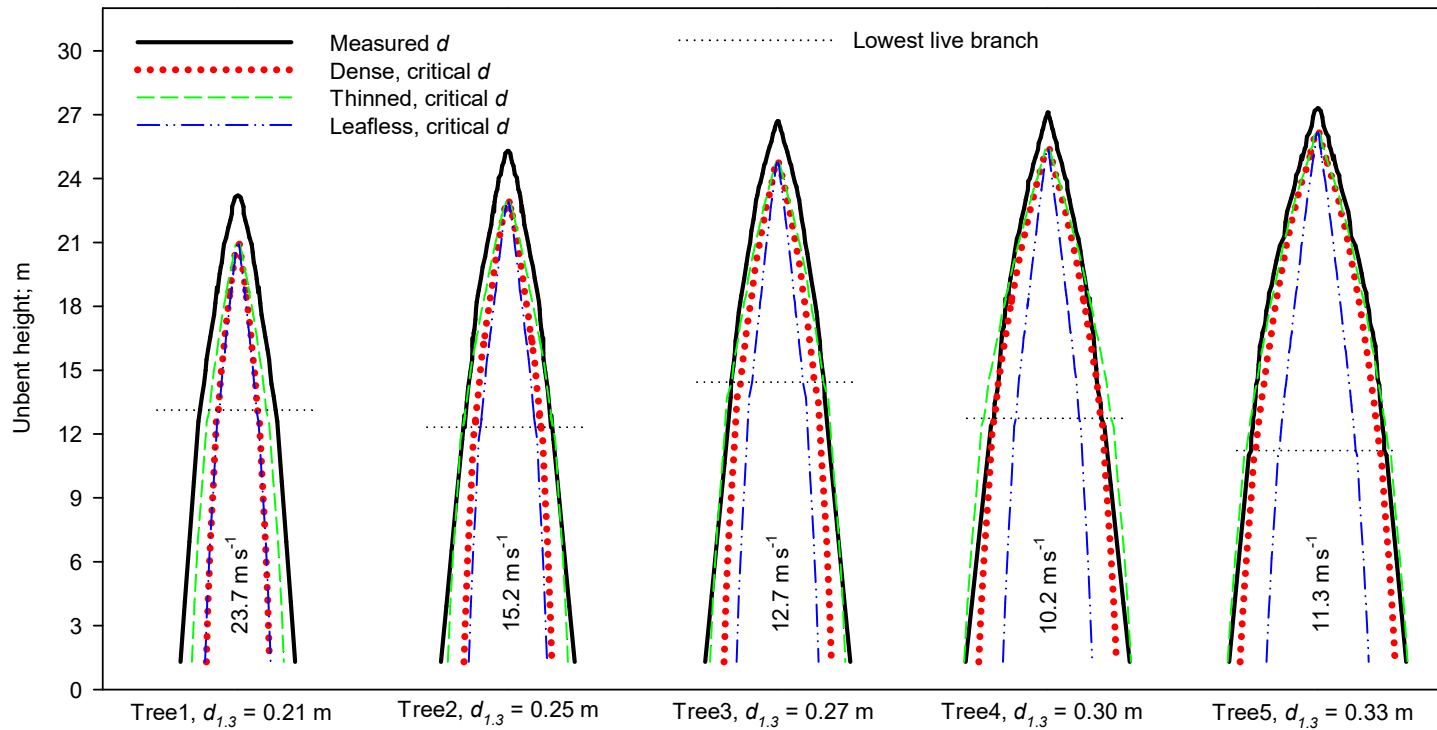


Figure 8. The dimensions of five felled tree trunks (solid black) and dimensions sufficient to withstand wind and gravity (dotted and dashed lines) in a meteorological situation that causes a mean wind above the canopy of the dense stand (w) of 10.2 m s^{-1} , which is the critical speed that nearly breaks Tree4. The heights on vertical axis and diameters on the horizontal axis are not proportional. Diameters at a height of 1.3 m

are given in the bottom. The critical above-canopy wind speed for the dense stand is indicated inside the trunks. The lowest living branches were at heights of 11.2–14.5 m.